JACS
JOURNAL OF THE AMERICAN CHEMICAL SOCIETY
Article
pubs.acs.org/JACS

Side-Chain-Induced Rigid Backbone Organization of Polymer Semiconductors through Semifluoroalkyl Side Chains

Boseok Kang,[†,∥] Ran Kim,[‡,∥] Seon Baek Lee,[†] Soon-Ki Kwon,[§] Yun-Hi Kim,[*,‡] and Kilwon Cho[*,†]

[†]Department of Chemical Engineering, Pohang University of Science and Technology, Pohang 790-784, Korea
[‡]Department of Chemistry and RIGET, Gyeongsang National University, 501 Jinju Daero, Jinju, 660-701, Korea
[§]School of Materials Science & Engineering and ERI, Gyeongsang National University, 501 Jinju Daero, Jinju, 660-701, Korea

Supporting Information

ABSTRACT: While high-mobility p-type conjugated polymers have been widely reported, high-mobility n-type conjugated polymers are still rare. In the present work, we designed semifluorinated alkyl side chains and introduced them into naphthalene diimide-based polymers (PNDIF-T2 and PNDIF-TVT). We found that the strong self-organization of these side chains induced a high degree of order in the attached polymer backbones by forming a superstructure composed of "backbone crystals" and "side-chain crystals". This phenomenon was shown to greatly enhance the ordering along the backbone direction, and the resulting polymers thus exhibited unipolar n-channel transport in field-effect transistors with remarkably high electron mobility values of up to 6.50 $cm^2 V^{-1} s^{-1}$ and with a high on−off current ratio of 10^5.

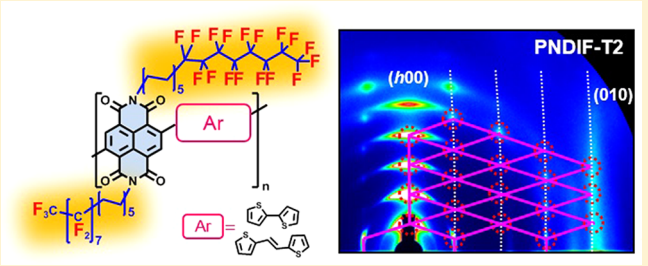

INTRODUCTION

π-Conjugated polymer semiconductors have been the subject of intense research in the past few decades because of their potential applications in low-cost large-area printed electronics including field-effect transistors (FETs), light-emitting diodes, and solar cells.[1−8] Compared to their inorganic counterparts, a distinctive feature of such polymeric semiconductors is their solution processability, which results from attached flexible side chains.[9] The appropriate selection and attachment of side chains involves the art of balancing several considerations, because the side chains may affect molecular packing, thin-film morphology, and hence performance of device materials, as well as afford a rigid π-conjugated backbone with the satisfactory solubility for purification and device fabrication.[10,11] Long branched alkyl chains, such as 2-hexyldecyl (HD), 2-octyldodecyl (OD), and 2-decyltetradecyl (DT) groups, have been typically introduced,[12−14] but their insulating and bulky natures have traditionally been considered to hamper charge transport in polymer films by hindering efficient intermolecular interactions.[15]

Fluoroalkyl chains are particularly of interest because of their unique properties, such as hydrophobicity, rigidity, and thermal stability, as well as chemical and oxidative resistance and their ability to self-organize.[9,10,16] Such unique properties suggest that fluoroalkyl chains may serve as promising solubilizing groups especially for n-type organic semiconductors. For example, the hydrophobicity and the closely packed structure of fluorinated alkyl chains have been found to prevent the diffusion of moisture and oxygen into films, thereby promiting the stability of the polymers in ambient air.[17,18] The high thermal stability of fluoroalkyl polymers would also be a favorable feature during device manufacturing.[19] Furthermore, the fluorophobic interactions present in fluorine-rich organic compounds often induce unique self-organized architectures and may facilitate charge transport in organic semiconductors by promoting strong intermolecular interactions.[20−22] However, despite such interesting characteristics, the introduction of fluoroalkyl chains in organic semiconductors has been less studied compared to the introduction of alkyl side chains and has been limited to a few small molecules[17,23−28] and polythiophenes.[21,29]

In the present study, we designed and synthesized high-electron-mobility air-stable semiconducting polymers with semifluoroalkyl side chains, and compared their microstructural characteristics with those of branched alkyl analogues. An electron-accepting naphthalene diimide (NDI) unit with a $-(CH_2)_{10}(CF_2)_7CF_3$ semifluoroalkyl chain was alternatively coupled with electron-donating bithiophene (T2) or thienylene-vinylene-thienylene (TVT) units to give two newly synthesized semiconducting polymers (Figure 1a). Both polymers, poly[2,7-bis(11,11,12,12,13,13,14,14,15,15,16,16,17,17,18,18,18-heptadecafluorooctadecyl)-4-methyl-9-(5′-methyl-[2,2′-bithiophen]-5-yl)benzo[*lmn*][3,8]phenanthroline-1,3,6,8(2*H*,7*H*)-tetraone] (PNDIF-T2) and [(*E*)-2,7-bis(11,11,12,12,13,13,14,14,15,15,16,16,17,17,18,18,18-heptadecafluorooctadecyl)-4-methyl-9-(5-(2-(5-methylthiophen-2-yl)-vinyl)thiophen-2-yl)benzo[*lmn*][3,8]phenanthroline-1,3,6,8-(2*H*,7*H*)-tetraone] (PNDIF-TVT), were found to be air-stable and showed superior crystalline order. Notably, we found that

Received: October 6, 2015
Published: December 11, 2015

DOI: 10.1021/jacs.5b10445
J. Am. Chem. Soc. 2016, 138, 3679−3686

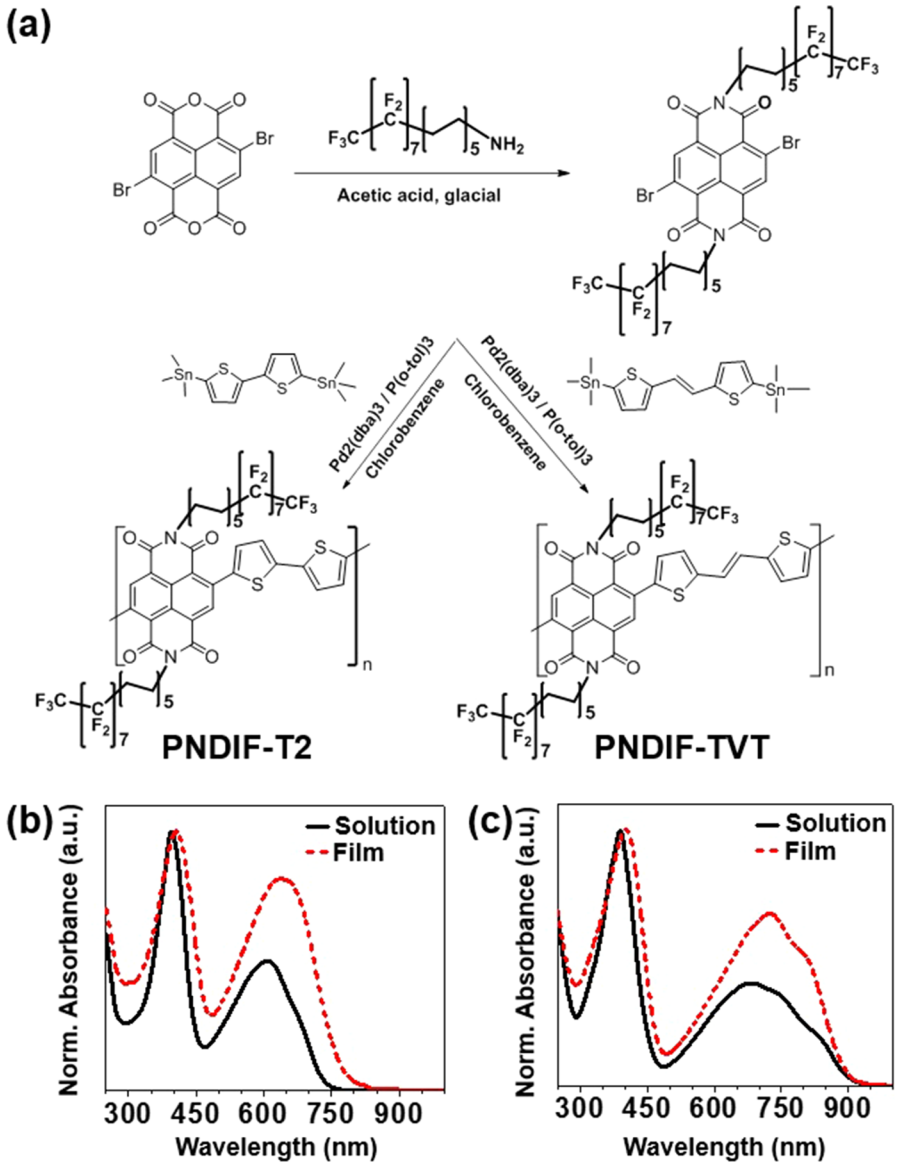

Figure 1. (a) Synthetic routes used to produce polymers with semifluorinated side chains. Normalized absorption spectra in solution ($CHCl_3$) and thin films of (b) PNDIF-T2 and (c) PNDIF-TVT polymers.

the strong self-organization of semifluoroalkyl segments resulted in a high degree of long-range order in polymer crystallites, inducing rigidity in the polymer backbones. These unique organizational features in the polymer thin films gave rise to a superior electron mobility of up to 6.5 $cm^2 V^{-1} s^{-1}$, far higher than those of polymers with branched alkyl chains. These results demonstrate the usefulness of semifluoroalkyl side chains in polymer semiconductor application.

RESULTS AND DISCUSSION

Two semiconducting polymers containing semifluoroalkyl side chains (PNDIF-T2/-TVT) were synthesized as shown schematically in Figure 1a. For comparison, two additional polymers with the same backbone but with branched alkyl side chains were also synthesized: PNDI2OD-T2 and PNDI2DT-TVT (their full names and chemical structures are provided in Figure S1 of the Supporting Information (SI)).[30,31] For the synthesis of the semifluoroalkyl substituent, first, heptadecafluorooctan-1-ol was prepared by electrophilic addition followed by reduction with a Zn catalyst. Heptadecafluorooctadecan-1-amine was obtained by Gabriel synthesis followed by tosylation and nucleophilic substitution. The imidization of dibromonaphthalene dianhydride and heptadecafluorooctadecan-1-amine was performed in acetic acid. PNDIF-T2 and PNDIF-TVT were synthesized by the Stille coupling reaction; detailed procedures are provided in the SI. The obtained polymers were purified by successive Soxhlet extraction with methanol, acetone, hexane, toluene, and chloroform. After these extractions, the polymer was reprecipitated into methanol. The structure of the monomer was confirmed by ^{1}H NMR, ^{13}C NMR, ^{19}F-NMR and HR-MS. The polymers were characterized by ^{1}H NMR (see the Synthesis section and Figures S2−S7 in the SI). Both polymers exhibited good solubility in common organic solvents such as chloroform and chlorobenzene owing to the flexibility of semifluoroalkyl side chains. The number-average molecular weights ($\overline{M_n}$) of the polymers were determined by gel permeation chromatography (GPC) analysis against polystyrene standards using chloroform as the solvent. PNDIF-T2 and PNDIF-TVT were shown to

DOI: 10.1021/jacs.5b10445
J. Am. Chem. Soc. 2016, 138, 3679−3686

Table 1. Physical Properties of the Polymers

polymers	$\overline{M_n}/\overline{M_n}$ (kDa)	T_d (°C)	λ_{max}^{sol} (nm)	λ_{max}^{film} (nm)	E_g (eV)[a]	E_{HOMO} (eV)[b]	E_{LUMO} (eV)[c]
PNDIF-T2	28/57	413	690	639	1.61	−5.62	−4.01
PNDIF-TVT	33/51	426	682	724	1.39	−5.38	−3.99

[a]Estimated from the onset of the UV−vis spectra. [b]$E_{HOMO} = E_{LUMO} - E_g$. [c]Onsets, potentials vs Fc/Fc^+ as external reference.

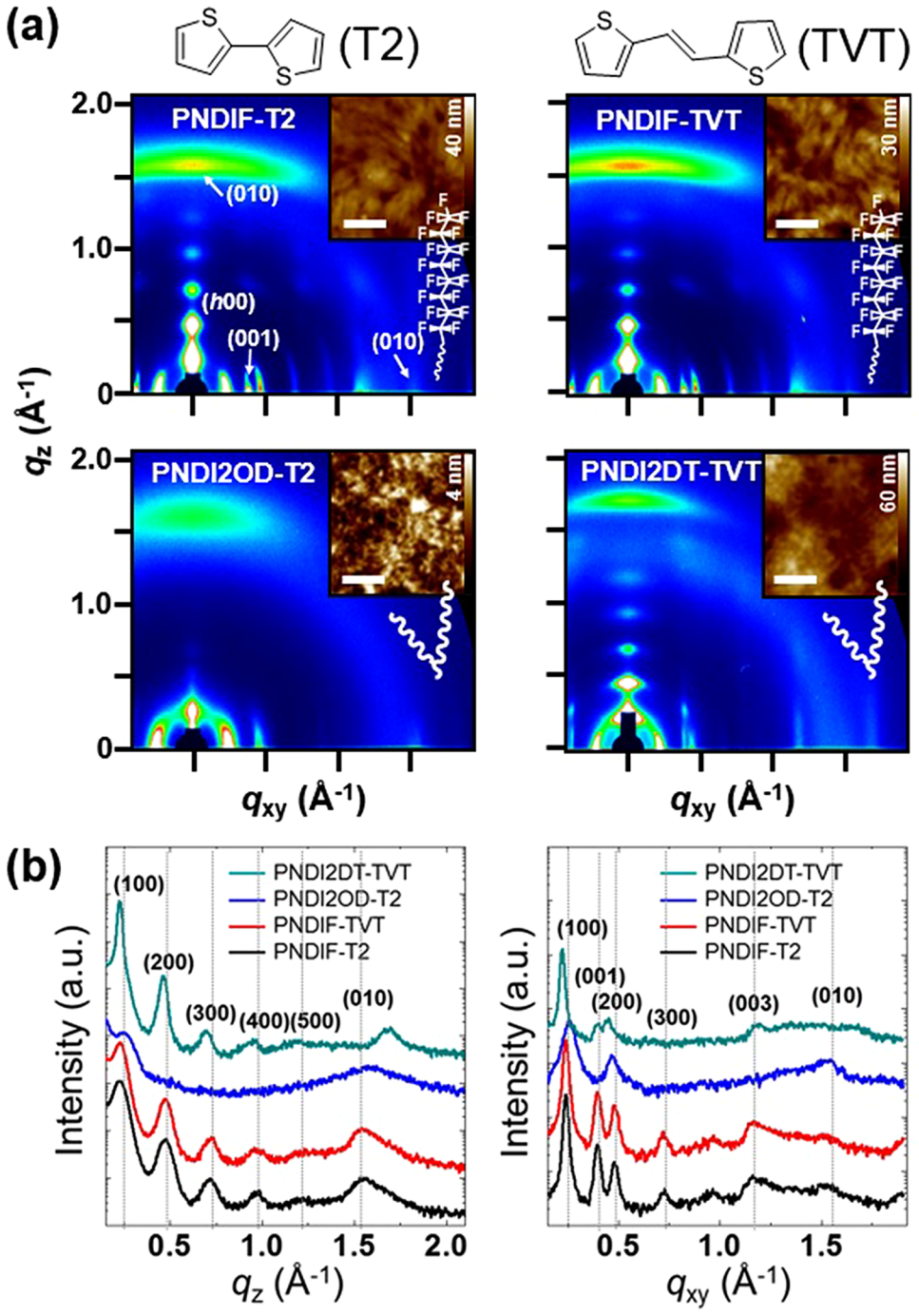

Figure 2. (a) 2D GIXD patterns of polymer thin films thermally annealed at 250 °C. The insets are the AFM height images of the corresponding thin films, where the scale bars are 500 nm. (b) The corresponding GIXD diffractogram profiles along the out-of-plane and in-plane directions.

have $\overline{M_n}$ values of 28 and 33 kDa with polydispersity indexes (PDIs) of 2.04 and 1.55, respectively.

The UV−vis absorption spectra of the two copolymers are shown in Figure 1b−c, and the optical, thermal, and electrochemical data are summarized in Table 1. The polymers showed typical dual-band absorption, where the band between 480 and 900 nm is a typical intramolecular charge transfer (ICT) absorption resulting from donor−acceptor structures of the polymers.[32] The optical band gaps (E_g, eV) of the polymers were calculated from the absorption edges and were found to

DOI: 10.1021/jacs.5b10445
J. Am. Chem. Soc. 2016, 138, 3679−3686

be 1.61 eV for PNDIF-T2 and 1.39 eV for PNDIF-TVT. The reduced E_g value of PNDIF-TVT compared to that of PNDIF-T2 was attributed to the extended π-conjugation in the polymer backbone, resulting from the incorporation of vinylene groups between the thiophene rings.[13,31] Cyclic voltammetry (CV) measurements of the two polymers in thin films were taken to evaluate their electronic energy levels (see Figure S8, SI). The highest occupied molecular orbital (HOMO) level of PNDIF-TVT (−5.38 eV) was found to be higher than that of PNDIF-T2 (−5.62 eV), which may again be due to the extended π-conjugation of PNDIF-TVT. The lowest unoccupied molecular orbital (LUMO) levels of both polymers were close to −4.0 eV, which is suitable for n-channel materials and assures the stability of the polymers in ambient air.[33]

Density functional theory (DFT) calculations performed using the B3LYP functional and a 6-31G* basis set showed the LUMOs of PNDIF-T2 and PNDIF-TVT to be substantially concentrated on the central NDI units (see Figures S9 and S10, SI).[31] The calculated energy gap of PNDIF-TVT was determined to be narrower than that of PNDIF-T2, consistent with the optical band gap results. Interestingly, compared with the branched alkyl side chains, the introduction of semifluoroalkyl side chains had relatively little effect on the energy levels and dihedral angles of the monomers (the angles between NDI and T2 or between NDI and TVT). These results indicated that the changes in electrical properties of the polymers upon introducing semifluoroalkyl side chains would mostly correlate with the changes in intermolecular interactions in the solid state, rather than with changes in the characteristics on the single-molecular level.[34]

The thermal properties of the polymers were investigated using thermogravimetric analysis (TGA) and differential scanning calorimetry (DSC) under a N_2 atmosphere (Table 1 and Figures S11−S12, SI). Both polymers exhibited good thermal stability, with 5% weight loss (T_d) over 400 °C. Furthermore, endothermic transition (T_m) peaks arose for the polymers at 284 °C (for PNDIF-T2) and 291 °C (for PNDIF-TVT), respectively, indicating both polymers to be semicrystalline. Importantly, the T_m of PNDIF-TVT was observed to be much higher than that of PNDI2TD-TVT (230 °C),[31] demonstrating that the introduction of semifluorinated alkyl chains in place of the hydrocarbon alkyl chains in the NDI unit enhanced the thermal stability of the polymer, which might be due to the strong organization properties of semifluorinated alkyl chains.[31]

The crystalline nature and molecular orientations of the polymers with semifluoroalkyl side chains were studied by two-dimensional grazing-incidence X-ray diffraction (2D GIXD) analysis. Figure 2a shows the 2D GIXD patterns of the thermally annealed (at 250 °C) polymer thin films on octadecyltrimethoxysilane (OTS)-treated Si substrates. The polymers with branched alkyl side chains, i.e., PNDI2OD-T2 and PNDI2DT-TVT, were compared together. The magnified 2D GIXD images with indexing of peaks are shown in the SI (Figures S13 and S14). 2D GIXD patterns and corresponding 1D diffractogram profiles of the as-spun polymer thin films are also provided in the SI (Figure S15). First, in the 2D GIXD patterns of all the polymer thin films, which were as-spun and thermally annealed, including the patterns of those films with semifluoroalkyl side chains and those with branched alkyl side chains, both the (h00) and (010) reflections were competitively observed along the out-of-plane direction, confirming that the texture of the films was bimodal, i.e., that face-on and edge-on crystallites coexisted (Figure 2b).[35] After thermal annealing, the (100) and (010) reflections along the out-of-plane direction became stronger simultaneously, indicating that the crystallinity of the films was improved, with their molecular orientations retained with respect to substrates. Aside from PNDI2OD-T2, the 2D GIXD patterns of the other three polymers showed clear (h00) reflections up to the fifth order for the out-of-plane direction and an intense (010) reflection for the in-plane direction, indicating the superior crystallinity of these polymers.[36] The high crystallinity indicated by the 2D GIXD images is consistent with the observed AFM morphologies (see the insets in Figure 2a). The root-mean-square roughness (R_{RMS}) values of the three polymer films were determined to be an order of magnitude higher than that of the PNDI2OD-T2 films (a full set of the AFM images at various annealing temperatures are shown in Figure S16 and S17, SI).[37] The most prominent difference between the polymers with branched alkyl and semifluoroalkyl side chains was the generation of intense (00l) reflections with q_z components by the latter. For the polymers with T2 units (PNDIF-T2 and PNDI2OD-T2), the (00l) reflections along the in-plane directions, which resulted from the rigidity of polymer backbones, newly appeared after replacing the branched alkyl side chains with linear semifluoroalkyl chains. For the polymers with TVT units (PNDIF-TVT and PNDI2DT-TVT), the (00l) reflections became clearer and more intense after this replacement of the side chains. The strong (00l) reflections showed that the attachment of the semifluoroalkyl side chains improved the crystalline order of the polymer thin films, in particular by increasing the rigidity of the main chains of the polymer.[36] The distinct (00l) reflections in the 2D GIXD images of the as-spun thin films of the polymers with the semifluoroalkyl side chains provided further for the improved rigidity afforded by semifluoroalkyl side chains, compared to those afforded by the branched-alkyl counterparts (Figure S15, SI).

To quantitatively analyze the thin-film crystalline structures, careful evaluations of the lamellar stacking, π−stacking, and backbone-direction d-spacings were carried out with the appropriate corrections.[38] All of the detailed structural results obtained from our 2D GIXD analysis are listed in Table S1 in the SI. The lamellar stacking, π−stacking, and backbone-direction d-spacings of PNDIF-T2 became identical to those of PNDIF-TVT after thermal annealing, with values of 27.4, 4.1, and 15.8 Å, respectively, regardless of the chemical structures of the donor units. These results strongly implied that the crystalline structures of the polymer thin films were dominantly governed by the strong self-organization of the fluoroalkyl chains, rather than by the interaction between the backbones. Furthermore, the π-stacking spacings of the polymers with TVT units increased from 3.8 to 4.1 Å as semifluoroalkyl side chains were incorporated, consistent with the minimum spacing between antiparallel semifluorocarbon segments being about 4.05 Å.[39] The lamellar d-spacing of 27.4 Å corresponds to approximately half of the length of the NDI unit with fully stretched semifluoroalkyl side chains (~54 Å), indicating a tight interdigitation of antiparallel semifluoroalkyl chains.

The electrical performances of the polymers were evaluated by fabricating bottom-gate/top-contact polymer FET (PFET) devices. The polymer thin films were prepared on OTS-treated SiO_2 (300 nm)/Si substrates by spin-casting a chloroform solution (7 mg mL^{-1}) of these films with or without the 1-chloronaphthalene (CN) solvent additive, and then carrying out thermal annealing for 20 min in a N_2 atmosphere, followed

DOI: 10.1021/jacs.5b10445
J. Am. Chem. Soc. 2016, 138, 3679−3686

by depositing the Au source and drain electrodes (channel length and width are 150 and 1500 μm, respectively). Figure 3a

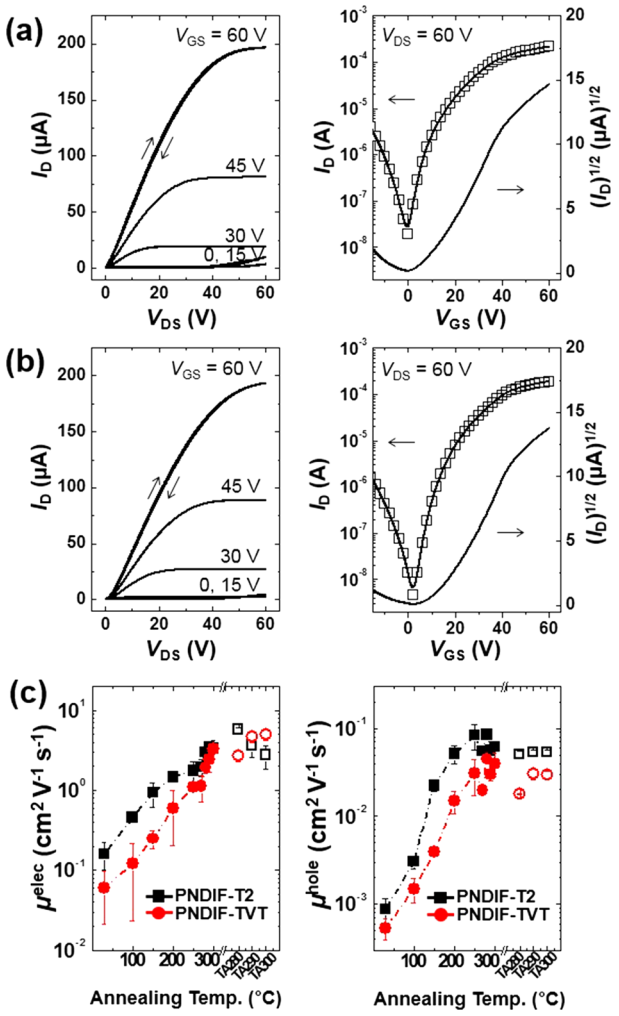

Figure 3. Current–voltage characteristics of PFETs. Output characteristics and transfer curves of PFETs based on (a) PNDIF-T2 and (b) PNDIF-TVT thin films prepared with a 1-chloronaphthalene (CN) solvent additive and thermally annealed at the optimized temperatures (280 °C for PNDIF-T2 and 300 °C for PNDIF-TVT). (c) Electron (μ^{elec}) and hole (μ^{hole}) mobilities as a function of annealing temperature, where closed and open symbols indicate those of the devices fabricated without or with the CN additive, respectively. For the CN-processed OFETs, the CN additive of 1.2 vol % was added to the polymer semiconductor–chloroform solution and the rest of the device fabrication was the same.

and 3b show the output and transfer characteristics of the optimized PFET devices. Both PNDIF-T2/-TVT exhibited unipolar n-channel field-effect behaviors, mainly due to the low-lying HOMO levels;[40,41] hole mobility values were observed to be 2 orders of magnitude lower than the electron mobility values. Thermal annealing resulted in significantly improved electron mobility values of both polymers, compared with the as-cast thin films (Figure 3c and Figure S18 in the SI). This result can be attributed to the improved crystalline ordering and enlarged crystalline domains after thermal annealing.[3,42] The performances of the devices based on these polymers are summarized in Table S3 in the SI.

The thermally annealed PNDIF-T2/-TVT films showed efficient n-channel operations with high electron mobility values of up to 3.93 and 3.75 cm^2 V^{-1} s^{-1}, respectively, and high on–off current ratios of 10^5 with superior ambient stability; the electrical characteristics of the annealed devices were almost unchanged after exposure to air for three months. The electron mobility values attained for these films were much higher than those of PNDI2OD-T2 and PNDI2DT-TVT (up to 0.1 and 1.84 cm^2 V^{-1} s^{-1} respectively; see Table S4 in the SI). The enhanced electron transport characteristics with semifluoroalkyl side chains can be mainly attributed to the enhanced backbone rigidity suggested in the quasi-1D charge-transport model,[34,36] because the π-stacking distance of the polymers of 4.1 Å is somewhat large and thus might be unfavorable for interchain charge transport.[40] We believe that these results are significant evidence for the importance of backbone rigidity in the charge transport of semiconducting polymers. It is noteworthy that bar-coated PNDI2OD-T2 films that have improved ordering along the conjugated backbones have recently shown very high electron mobilities of up to 6.4 cm^2 V^{-1} s^{-1} at the aligned direction, possibly supporting the charge transport model.[43] Furthermore, we tested the bias-stress stability of fabricated PFETs, where the PFETs with PNDIF-T2/-TVT exhibited more stable operation than did the PNDI2OD-T2 and PNDI2DT-TVT FETs. The better bias-stress stability of PFETs with PNDIF-T2/-TVT is presumably attributed to the aforementioned superior crystalline order and the difference in the chemical structure of the side chains (see the detailed results in Figure S19, SI).[44]

In addition to the thermal annealing process, the CN solvent additive, an organic solvent with a high boiling point of 259 °C,[37] was introduced with the aim of further enhancing the performances of the PFETs. The CN-processed PNDIF-T2 and PNDIF-TVT FETs displayed considerably enhanced electron mobilities of up to 6.50 and 5.64 cm^2 V^{-1} s^{-1}, respectively (average values of 5.73 and 4.92 cm^2 V^{-1} s^{-1}). To explain the significantly better performance of the CN-processed PFETs, we examined the crystalline structures and morphologies of the polymer films prepared with or without the CN additive and annealed at 280 °C (Figure 4a and b). In striking contrast to the bimodal texture of the films without CN described above, the CN-processed films have a predominantly edge-on texture. The dramatic change in texture may, therefore, have been largely responsible for the improvement of the mobility, because optimal PFET performance is often achieved when π-stacking is mostly aligned parallel to the substrate.[45−48] The superior long-range order of the CN-processed films, as indicated by the stronger reflections in the 2D GIXD patterns and increased R_{RMS} values in the AFM images (Figure S20, SI), may also have contributed to the significantly better performance of the CN-processed PFETs.[2,49]

Furthermore, the extension of main chains along the polymer's backbone direction can facilitate the electron transport.[50] The DFT calculated lengths of the repeating units in PNDIF-T2 and PNDIF-TVT are quite different, at 14.3 and 16.8 Å, respectively (Figure S9, SI), but the same *d*-spacings along the backbone direction (15.8 Å) were observed in the 2D GIXD experiments (Table S1, SI). Specifically, in the case of PNDIF-T2, the DFT-calculated repeating unit length of the polymer is much shorter than the backbone-direction *d*-spacing (14.3 Å < 15.8 Å), indicating that the polymer chains should be extended along that direction when they are in a solid state. Interestingly, the *d*-spacings along the backbone direction increased from 15.9 to16.2 Å with the use of CN additives, implying a further lengthening (see Table S2, SI). An extension

DOI: 10.1021/jacs.5b10445
J. Am. Chem. Soc. 2016, 138, 3679−3686

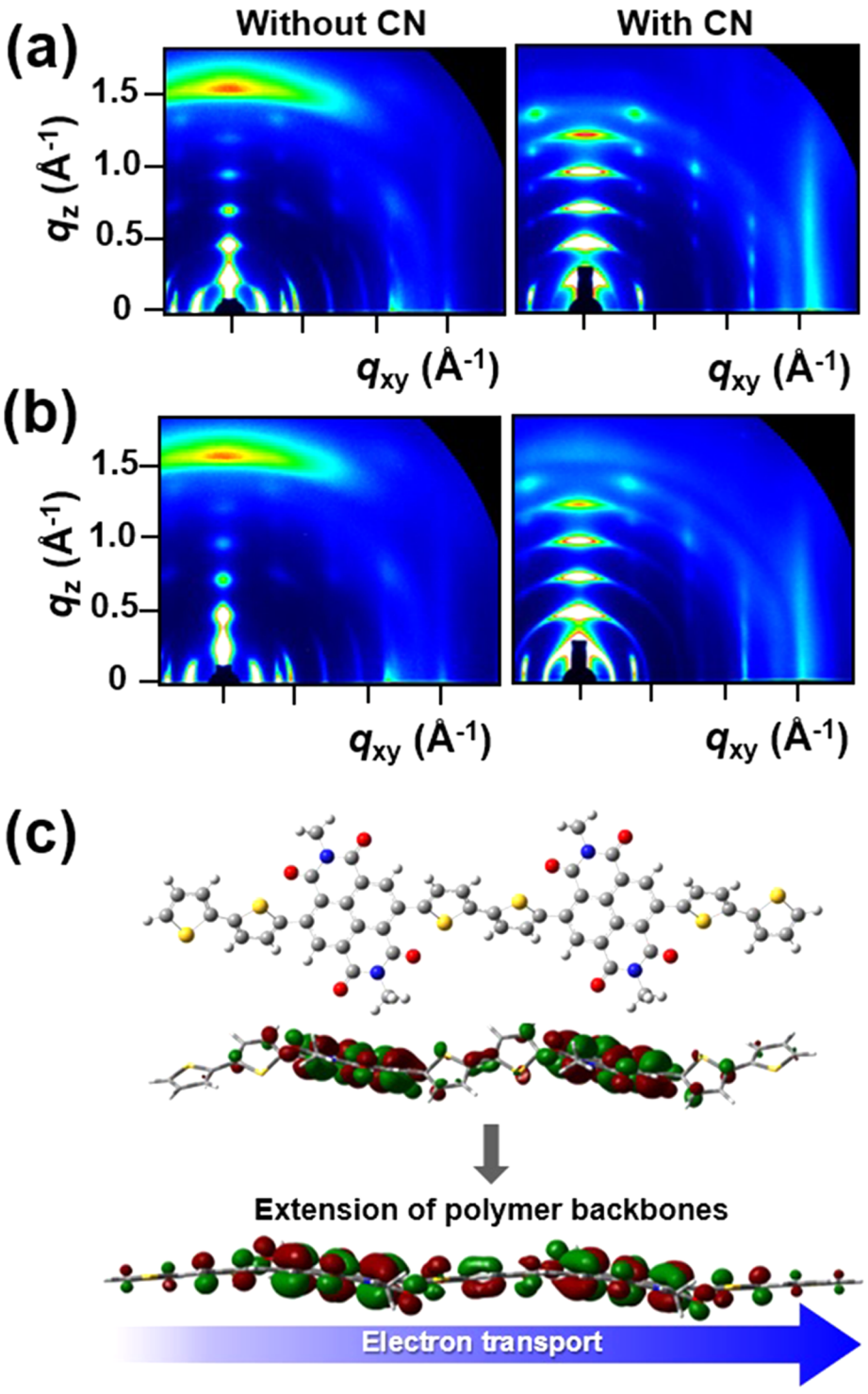

Figure 4. 2D GIXD patterns of (a) PNDIF-T2 and (b) PNDIF-TVT thin films that were prepared with/without the CN additive and thermally annealed at 280 °C. (c) Results of the DFT calculations of the molecular structures and their lowest unoccupied molecular orbitals (LUMOs) (top) in the optimized geometry and (bottom) in the extended geometry along the backbone direction.

of the polymer chain along the backbone direction would cause changes of the dihedral angles between the repeating units and thus of the frontier orbitals as well. An extension could cause the LUMOs of the polymer to become more delocalized across the conjugated backbone (Figure 4c), thereby leading to the better intramolecular electron-transport characteristics.[50,51] The strong self-organization of semifluoroalkyl segments through fluorophobic interactions may contribute to such a backbone extension.[21] This conjecture is evidenced by the distinct hexagonal patterns observed in the 2D GIXD patterns of the CN-processed films (Figures 4a and 4b), because the semifluoroalkyl segments can form the closely packed hexagonal-like structure, as previously suggested in semi-fluorinated *n*-alkanes (magnified 2D GIXD images are provided in the SI, Figure S21).[39] Scheme 1 shows a suggested crystalline structure of PNDIF-T2, which appears like a superstructure

DOI: 10.1021/jacs.5b10445
J. Am. Chem. Soc. 2016, 138, 3679−3686

Scheme 1. Schematic of Molecular Packing of PNDIF-T2 and Its Side Chains Based on Data from X-ray Scattering and DFT Calculations[a]

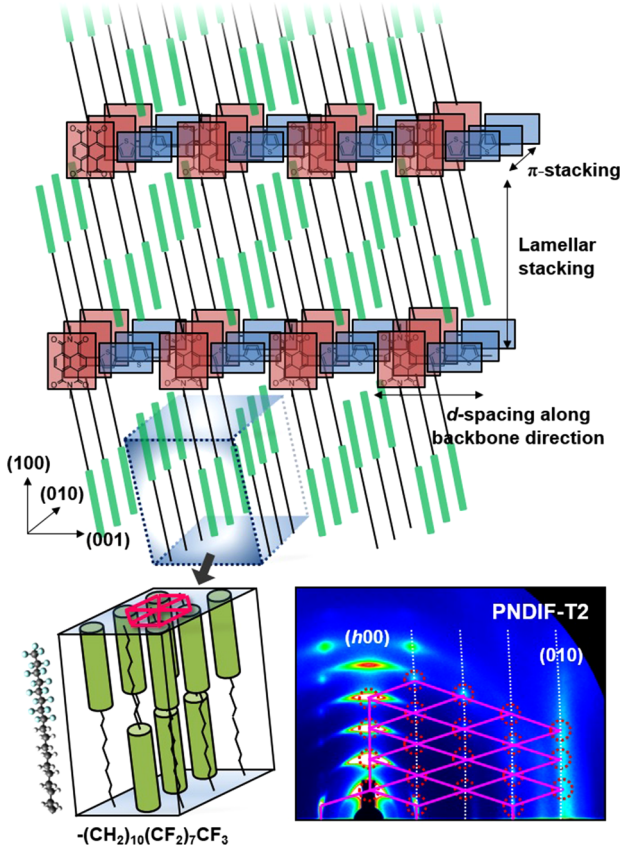

[a]The positions of the molecules are qualitative and are not meant to quantitatively describe the details of the molecular packing. The 2D GIXD pattern of CN-processed PNDIF-T2 clearly reveals a hexagonal packing structure of semifluoroalkyl side chains.

consisting of conjugated backbone crystals within a crystal of fluoroalkanes in light of their volume ratio (backbone crystal ~30%).

CONCLUSIONS

In summary, semifluorinated alkyl side chains were designed and synthesized with n-type NDI-based copolymers (PNDIF-T2 and PNDIF-TVT). The introduction of the semifluoroalkyl side chains not only endowed the rigid polymer backbones with satisfactory solubility but also led to superior microstructural ordering of the attached polymer chains through the strong self-organization of the side chains themselves. Unipolar n-channel charge-transport behaviors were observed for the resulting copolymers. In particular, PNDIF-T2 showed a remarkably high electron mobility of up to 6.50 $cm^2 V^{-1} s^{-1}$ with a high on−off current ratio of 10^5. These results shed new light on the usefulness of semifluorinated alkyl side chains for organic semiconductor materials. We believe that our findings on the side-chain induced rigid backbone organization will provide a useful guide to optimize the solid state packing and electrical properties of high-mobility semiconducting polymers.

ASSOCIATED CONTENT

Supporting Information

The Supporting Information is available free of charge on the ACS Publications website at DOI: 10.1021/jacs.5b10445.

Detailed experimental procedures and characterizations for polymers as well as the device fabrication procedures, measurements, and additional figures (Tables S1−S4 and Figures S1−S21) (PDF)

AUTHOR INFORMATION

Corresponding Authors

*E-mail: ykim@gnu.ac.kr (Y.K.).
*E-mail: kwcho@postech.ac.kr (K.C.).

Author Contributions

‖B.K. and R.K. contributed equally.

Notes

The authors declare no competing financial interest.

ACKNOWLEDGMENTS

The authors thank the Pohang Accelerator Laboratory for providing the synchrotron radiation sources at 3C and 9A beamlines used in this study. This work was supported by a grant (Code No. 2011-0031628) from the Center for Advanced Soft Electronics under the Global Frontier Research Program of the Ministry of Science, ICT and Future Planning, Korea, and the National Research Foundation of Korea (NRF) grant funded by the Korea government (MSIP) (2015R1A2A1A10055620).

REFERENCES

(1) Sirringhaus, H.; Brown, P. J.; Friend, R. H.; Nielsen, M. M.; Bechgaard, K.; Langeveld-Voss, B. M. W.; Spiering, A. J. H.; Janssen, R. A. J.; Meijer, E. W.; Herwig, P.; de Leeuw, D. M. *Nature* **1999**, *401*, 685.
(2) McCulloch, I.; Heeney, M.; Bailey, C.; Genevicius, K.; MacDonald, I.; Shkunov, M.; Sparrowe, D.; Tierney, S.; Wagner, R.; Zhang, W. M.; Chabinyc, M. L.; Kline, R. J.; Mcgehee, M. D.; Toney, M. F. *Nat. Mater.* **2006**, *5*, 328.
(3) Kline, R. J.; Mcgehee, M. D.; Toney, M. F. *Nat. Mater.* **2006**, *5*, 222.
(4) Kang, B.; Lee, W. H.; Cho, K. *ACS Appl. Mater. Interfaces* **2013**, *5*, 2302.
(5) Cho, J. H.; Lee, J.; Xia, Y.; Kim, B.; He, Y. Y.; Renn, M. J.; Lodge, T. P.; Frisbie, C. D. *Nat. Mater.* **2008**, *7*, 900.
(6) Kang, B.; Jang, M.; Chung, Y.; Kim, H.; Kwak, S. K.; Oh, J. H.; Cho, K. *Nat. Commun.* **2014**, *5*, 4752.
(7) Chou, K. W.; Yan, B. Y.; Li, R. P.; Li, E. Q.; Zhao, K.; Anjum, D. H.; Alvarez, S.; Gassaway, R.; Biocca, A.; Thoroddsen, S. T.; Hexemer, A.; Amassian, A. *Adv. Mater.* **2013**, *25*, 1923.
(8) Hunter, S.; Chen, J. H.; Anthopoulos, T. D. *Adv. Funct. Mater.* **2014**, *24*, 5969.
(9) Lei, T.; Wang, J. Y.; Pei, J. *Chem. Mater.* **2014**, *26*, 594.
(10) Mei, J. G.; Bao, Z. N. *Chem. Mater.* **2014**, *26*, 604.
(11) Niebel, C.; Kim, Y. G.; Ruzie, C.; Karpinska, J.; Chattopadhyay, B.; Schweicher, G.; Richard, A.; Lemaur, V.; Olivier, Y.; Cornil, J.; Kennedy, A. R.; Diao, Y.; Lee, W. Y.; Mannsfeld, S.; Bao, Z. N.; Geerts, Y. H. *J. Mater. Chem. C* **2015**, *3*, 674.
(12) Lei, T.; Cao, Y.; Zhou, X.; Peng, Y.; Bian, J.; Pei, J. *Chem. Mater.* **2012**, *24*, 1762.
(13) Chen, H. J.; Guo, Y. L.; Mao, Z. P.; Yu, G.; Huang, J. Y.; Zhao, Y.; Liu, Y. Q. *Chem. Mater.* **2013**, *25*, 4835.
(14) Osaka, I.; Kakara, T.; Takemura, N.; Koganezawa, T.; Takimiya, K. *J. Am. Chem. Soc.* **2013**, *135*, 8834.

DOI: 10.1021/jacs.5b10445
J. Am. Chem. Soc. 2016, 138, 3679−3686

(15) Kang, I.; Yun, H. J.; Chung, D. S.; Kwon, S. K.; Kim, Y. H. *J. Am. Chem. Soc.* **2013**, *135*, 14896.
(16) Cheng, X. H.; Prehm, M.; Das, M. K.; Kain, J.; Baumeister, U.; Diele, S.; Leine, D.; Blume, A.; Tschierske, C. *J. Am. Chem. Soc.* **2003**, *125*, 10977.
(17) Katz, H. E.; Lovinger, A. J.; Johnson, J.; Kloc, C.; Siegrist, T.; Li, W.; Lin, Y. Y.; Dodabalapur, A. *Nature* **2000**, *404*, 478.
(18) Oh, J. H.; Suraru, S. L.; Lee, W. Y.; Konemann, M.; Hoffken, H. W.; Roger, C.; Schmidt, R.; Chung, Y.; Chen, W. C.; Wurthner, F.; Bao, Z. N. *Adv. Funct. Mater.* **2010**, *20*, 2148.
(19) Hong, X. Y.; Tyson, J. C.; Middlecoff, J. S.; Collard, D. M. *Macromolecules* **1999**, *32*, 4232.
(20) Clark, C. G.; Floudas, G. A.; Lee, Y. J.; Graf, R.; Spiess, H. W.; Mullen, K. *J. Am. Chem. Soc.* **2009**, *131*, 8537.
(21) Jeong, H. G.; Lim, B.; Khim, D.; Han, M.; Lee, J.; Kim, J.; Yun, J. M.; Cho, K.; Park, J. W.; Kim, D. Y. *Adv. Mater.* **2013**, *25*, 6416.
(22) Huang, Y. C.; Welch, G. C.; Bazan, G. C.; Chabinyc, M. L.; Su, W. F. *Chem. Commun.* **2012**, *48*, 7250.
(23) Facchetti, A.; Deng, Y.; Wang, A. C.; Koide, Y.; Sirringhaus, H.; Marks, T. J.; Friend, R. H. *Angew. Chem., Int. Ed.* **2000**, *39*, 4547.
(24) Chikamatsu, M.; Itakura, A.; Yoshida, Y.; Azumi, R.; Yase, K. *Chem. Mater.* **2008**, *20*, 7365.
(25) Jones, B. A.; Ahrens, M. J.; Yoon, M. H.; Facchetti, A.; Marks, T. J.; Wasielewski, M. R. *Angew. Chem., Int. Ed.* **2004**, *43*, 6363.
(26) Weitz, R. T.; Amsharov, K.; Zschieschang, U.; Villas, E. B.; Goswami, D. K.; Burghard, M.; Dosch, H.; Jansen, M.; Kern, K.; Klauk, H. *J. Am. Chem. Soc.* **2008**, *130*, 4637.
(27) Facchetti, A.; Mushrush, M.; Yoon, M. H.; Hutchison, G. R.; Ratner, M. A.; Marks, T. J. *J. Am. Chem. Soc.* **2004**, *126*, 13859.
(28) Lv, A. F.; Li, Y.; Yue, W.; Jiang, L.; Dong, H. L.; Zhao, G. Y.; Meng, Q.; Jiang, W.; He, Y. D.; Li, Z. B.; Wang, Z. H.; Hu, W. P. *Chem. Commun.* **2012**, *48*, 5154.
(29) Wang, B.; Watt, S.; Hong, M.; Domercq, B.; Sun, R.; Kippelen, B.; Collard, D. M. *Macromolecules* **2008**, *41*, 5156.
(30) Yan, H.; Chen, Z. H.; Zheng, Y.; Newman, C.; Quinn, J. R.; Dotz, F.; Kastler, M.; Facchetti, A. *Nature* **2009**, *457*, 679.
(31) Kim, R.; Amegadze, P. S. K.; Kang, I.; Yun, H. J.; Noh, Y. Y.; Kwon, S. K.; Kim, Y. H. *Adv. Funct. Mater.* **2013**, *23*, 5719.
(32) Zhang, G. B.; Li, P.; Tang, L. X.; Ma, J. X.; Wang, X. H.; Lu, H. B.; Kang, B.; Cho, K.; Qiu, L. Z. *Chem. Commun.* **2014**, *50*, 3180.
(33) Anthony, J. E.; Facchetti, A.; Heeney, M.; Marder, S. R.; Zhan, X. W. *Adv. Mater.* **2010**, *22*, 3876.
(34) Kim, B. G.; Jeong, E. J.; Chung, J. W.; Seo, S.; Koo, B.; Kim, J. S. *Nat. Mater.* **2013**, *12*, 659.
(35) Beaujuge, P. M.; Frechet, J. M. J. *J. Am. Chem. Soc.* **2011**, *133*, 20009.
(36) Zhang, X. R.; Bronstein, H.; Kronemeijer, A. J.; Smith, J.; Kim, Y.; Kline, R. J.; Richter, L. J.; Anthopoulos, T. D.; Sirringhaus, H.; Song, K.; Heeney, M.; Zhang, W. M.; McCulloch, I.; DeLongchamp, D. M. *Nat. Commun.* **2013**, *4*, 2238.
(37) Kim, R.; Kang, B.; Sin, D. H.; Choi, H. H.; Kwon, S. K.; Kim, Y. H.; Cho, K. *Chem. Commun.* **2015**, *51*, 1524.
(38) Kim, H. G.; Kang, B.; Ko, H.; Lee, J.; Shin, J.; Cho, K. *Chem. Mater.* **2015**, *27*, 829.
(39) Tamada, K.; Ishida, T.; Knoll, W.; Fukushima, H.; Colorado, R.; Graupe, M.; Shmakova, O. E.; Lee, T. R. *Langmuir* **2001**, *17*, 1913.
(40) Klauk, H. *Chem. Soc. Rev.* **2010**, *39*, 2643.
(41) Zaumseil, J.; Sirringhaus, H. *Chem. Rev.* **2007**, *107*, 1296.
(42) Yamashita, Y.; Tsurumi, J.; Hinkel, F.; Okada, Y.; Soeda, J.; Zajaczkowski, W.; Baumgarten, M.; Pisula, W.; Matsui, H.; Mullen, K.; Takeya, J. *Adv. Mater.* **2014**, *26*, 8169.
(43) Bucella, S. G.; Luzio, A.; Gann, E.; Thomsen, L.; McNeill, C. R.; Pace, G.; Perinot, A.; Chen, Z. H.; Facchetti, A.; Caironi, M. *Nat. Commun.* **2015**, *6*, 8394.
(44) Lee, W. H.; Choi, H. H.; Kim, D. H.; Cho, K. *Adv. Mater.* **2014**, *26*, 1660.
(45) Zhang, X. R.; Richter, L. J.; DeLongchamp, D. M.; Kline, R. J.; Hammond, M. R.; McCulloch, I.; Heeney, M.; Ashraf, R. S.; Smith, J. N.; Anthopoulos, T. D.; Schroeder, B.; Geerts, Y. H.; Fischer, D. A.; Toney, M. F. *J. Am. Chem. Soc.* **2011**, *133*, 15073.
(46) Liu, F.; Wang, C.; Baral, J. K.; Zhang, L.; Watkins, J. J.; Briseno, A. L.; Russell, T. P. *J. Am. Chem. Soc.* **2013**, *135*, 19248.
(47) Chen, M. S.; Lee, O. P.; Niskala, J. R.; Yiu, A. T.; Tassone, C. J.; Schmidt, K.; Beaujuge, P. M.; Onishi, S. S.; Toney, M. F.; Zettl, A.; Frechet, J. M. J. *J. Am. Chem. Soc.* **2013**, *135*, 19229.
(48) Kim, D. H.; Park, Y. D.; Jang, Y. S.; Yang, H. C.; Kim, Y. H.; Han, J. I.; Moon, D. G.; Park, S. J.; Chang, T. Y.; Chang, C. W.; Joo, M. K.; Ryu, C. Y.; Cho, K. *Adv. Funct. Mater.* **2005**, *15*, 77.
(49) Mas-Torrent, M.; Rovira, C. *Chem. Rev.* **2011**, *111*, 4833.
(50) Noriega, R.; Salleo, A.; Spakowitz, A. J. *Proc. Natl. Acad. Sci. U. S. A.* **2013**, *110*, 16315.
(51) Zade, S. S.; Bendikov, M. *Chem. - Eur. J.* **2007**, *13*, 3688.

DOI: 10.1021/jacs.5b10445
J. Am. Chem. Soc. 2016, 138, 3679−3686